ACIDIC PRECIPITATION IN ONTARIO STUDY

LAGRANGIAN MODEL OF THE LONG RANGE TRANSPORT OF SULPHUR OXIDES

APIOS REPORT
No. 008/82

by

G. Ellenton, B. Ley, and P. K. Misra

Atmospheric Model Unit
Air Quality and Meteorology Section
Air Resources Branch
880 Bay Street
Toronto, Ontario, Canada

September, 1982

A.P.I.O.S. Coordination Office
Ontario Ministry of Environment
6th Floor, 40 St. Clair Ave. W.
Toronto, Ontario, Canada M4V 1M2
Project Coordinator: E. W. Piché

API 008/82
ISBN 0-7743-7269-9

1. Introduction

The transport of pollutants over long distances through the atmosphere has aroused concern because the depositon of pollutants and the ambient air quality far downstream may reach harmful levels when the effects of many sources are added together.

In this model of long range transport, the distances for which simulation is calculated are of the order 100 to 1000 km horizontally and one km vertically. Continuous emissions from a point source are modelled as a series of discrete puffs travelling successively along a wind flow trajectory which changes in time and space during the travel period. Chemical transformations of the pollutant and mass decay by loss to the earth's surface under wet and dry conditions are calculated along each trajectory. Summation of these processes over all trajectories for all emission sources yields concentration and deposition statistics at locations downstream.

The trajectory simulations constitute the core of the model. Over an extended period of time, one or two years, these trajectories may be considered to form a statistical ensemble representing long term average flow patterns for the pollutant.

The general form of the model permits the computation of mass budgets for any pollutant if the chemistry and the loss parameters can be ascertained. Currently the sulphur balance is being simulated

since sulphur ranks first in concern and has parameters which are probably the best known and most readily computed.

For long range transport, detailed fields near the source are not simulated. Each puff of pollutant is considered to be dispersed instantaneously in the vertical through the mixing layer. For calculation of a long term average (1-2 years) horizontal dispersion is simulated by the spread of the set of trajectories viewed as a whole rather than along individual trajectories. However, for simulation on a shorter time scale, such as a month, an episode or a day, there are not enough trajectories to create this dispersion. Hence it is necessary to apply horizontal disperson to the model calculations for simulation of short time periods.

The model is applied over a section of eastern North American centred on the Great Lakes, on a grid array of 23 x 26 points with a horizontal grid distance of 127 km. Currently the duration of trajectories is forty-eight hours.

The theory and development of this model has already been described (Atmospheric Model Development Unit; 1980), with a preliminary application to a sulphate episode period.

1.1 Comparison with Statistical Model

The Statistical model (Venkatram et al, 1981) is a simple but efficient model which calculates long term averages based on statistics of wind flow, chemical transformation and deposition. To compute annual average ambient concentration and depositions of pollutants, the model assumes a single average transport wind with a typical dispersion pattern. Statistical values of dry and wet duration times determine deposition during transport. In contrast, the Lagrangian model uses observed atmospheric pressures and precipitation at each time interval (e.g. every 6 hours) for many locations within the area of concern, i.e., eastern North America.

Thus the Lagrangian model can give results for shorter time periods such as a season, month, or possibly episode (4-5 days). The Lagrangian model traces the life history of each 6 hour 'packet' of emission from every source through the interactions along the flow, to its deposition on the earth's surface. However, the model is subject to uncertainties in wind computation and gross simplification of the physical and chemical influences during transport. Hence the effects must be computed as an average over many trajectories. Nevertheless, the averaging period can be as short as a few days if a sufficient number of trajectories are used and if suitable paramatric values are known.

The Lagrangian model, being much more complex than the Statistical model, is more expensive. It takes longer to develop, requires a large meteorological data set and more computer time for its operation. In return, the Lagrangian model can compute monthly or episode values which the Statistical model cannot do. It can compute year to year variations for each month, thereby showing trends in concentration and deposition values at different locations. The Lagrangian model can also build up a bank of trajectory data to provide dispersion statistics needed by the Statistical model.

In the report which follows, trajectory calculations are described in section 2, while mass balance of sulphur is detailed in section 3. The current state of the model is given in section 4, with projections of its operation for the near future. Results of preliminary tests are discussed, including a one month simulation for July 1979 and a simulation for the full year 1979. Recommendations for future modification to the model are made in section 5, with discussion of boundary layer winds, wet and dry depositions and reference to vertical dispersion and boundary layer height.

2. Trajector, Calculations

Horizontal trajectories are calculated within the mixed layer where the simulated wind speed and direction represent vertically averaged values within the layer. The advecting winds are geostrophic values computed from the surface pressure field and modified as to speed and direction to take into account the effect of surface friction and thermal stability. The reason for using surface pressures in preference to 850 mb values for the wind calculations as is often done, is that the time and space scales of pressure observations at the surface are the finest scale available. Surface pressures are reported hourly and six hourly at stations located roughly 100 km to 200 km apart. In contrast, 850 mb pressure observations are made every twelve hours at stations located 300 to 1000 km apart.

In order to create a pressure field which varies smoothly in space, orthogonal polynomials are fitted to the pressure data using a least squares fit criterion as given by Sykes and Hatton (1976).

In the boundary layer, surface friction is of comparable magnitude with pressure gradient and Coriolis forces. Hence boundary layer winds maintain a balance among these three forces. The geostrophic relation, while convenient for computing winds, takes into account the balance between only two forces, the pressure gradient and Coriolis. Surface friction reduces the wind speed from the geostrophic value. This causes turning in the anticlockwise direction from the geostrophic flow, or backing, such that the wind flows down the pressure gradient. The magnitude of these modifications due to surface friction depends on the turbulence in the boundary layer. In the model, for stable conditions, the wind

speed is reduced by 10% and the backing angle is 20°; for unstable conditions, the wind speed is geostrophic and the turning angle is 10°. Unstable conditions are assumed to prevail in the daytime and stable conditions at night. Discussion of more detailed calculations possible in the future is given in section 5.1.

Each trajectory is modelled in segments by wind vectors calculated from the pressure field at each time step Δt. Constant acceleration along each segment is maintained using the predictor-corrector method of Pettersen (1956). This is a relaxation adjustment between the wind vectors at each end of the segment at a given time, t. A new trajectory is started at the source point at each time interval. For example, for six-hour intervals, each forty-eight hour trajectory consists of eight six-hour segments and a new trajectory is started from the source point every six hours. These calculations are carried out for every source point.

Because of the random variation of the pressure field both spatially and temporally, each trajectory is unique. In this way the model calculates a collection of trajectories which can be regarded as a statistical ensemble of particle paths in a field of turbulence providing the set is large enough, i.e. if calculated for an extended period of time, at least one or two years.

Many simplifying assumptions underly the model, neglecting small scale complex variations. Consequently trajectories should not be considered to represent reality individually, but in total, as a long term average. Mass balance calculations, as described in the next section, are performed along each trajectory. The result is a long term average of pollutant distribution due to the trajectories.

3. Mass Balance

Continuous emission from each source is modelled as a series of discrete puffs. Each puff is assumed to fill instantaneously a grid volume 127 x 127 km^2 horizontally from the surface to the top of the mixing layer. Each puff then travels along a trajectory as calculated in section 2.

Concentrations of sulphur dioxide, q and sulphate, s along the trajectory are calculated by linear equations which express concentration as a decay function.

For sulphur dioxide,

$$\frac{dq}{dt} = -(k_d + k_w + k_t)\, q \qquad (1)$$

For sulphate

$$\frac{ds}{dt} = -(\bar{k}_d + \bar{k}_w)\, s + 3/2\, k_t\, q. \qquad (2)$$

Here k_d and $\bar{k}_d$ are dry deposition factors for sulphur dioxide and sulphate respectively. Similarly k_w and $\bar{k}_w$ are wet deposition factors. Chemical transformation of sulphur dioxide to sulphate is calculated using the factor k_t. This is expressed as a loss in equation (1) and a gain in equation (2). The proportion 3/2 is the ratio of the molecular weight of the two sulphur forms. This type of mass balance calculation is used in many models e.g. Eliassen and Saltbones (1975) and Bhumralkar et al (1981).

For a simple treatment, the k parameters are assumed independent of the concentration. Hence equations (1) and (2) are linear and may be integrated analytically. Since the value of k_w and $\bar{k}_w$ can change from one time step to another depending on whether rain is occurring, the analytical solution applies at each time step

individually and not over the whole trajectory. Integrating over the interval t to (t + Δ t),

$$q(t + \Delta t) = q(t) \exp(-K_1 \Delta t) \quad (3)$$

$$s(t + \Delta t) = s(t) \exp(-K_2 \Delta t) + \frac{q(t).3/2\, k_t}{2(K_1-K_2)} \exp(-K_2 \Delta t).$$

$$(1-\exp(-(K_1-K_2)\Delta t) \quad (4)$$

$$\text{At } t=0, \quad q(0) = \frac{Q}{H} (1-\alpha-\beta) \quad (5)$$

$$\text{and} \quad s(0) = 3/2\,\beta \frac{Q}{H} \quad (6)$$

In eqs. (3) and (4)

$$K_1 = k_d + k_w + k_t$$

and $K_2 = \bar{k}_d + \bar{k}_w$.

Q is the emission of sulphur per unit area, H is the mixed layer height. The factor α is the fraction of sulphur dioxide deposited locally (in the same grid square as the emission point) and β is the fraction of emission occurring as sulphate. Equations (3) and (4) are computed at each segment end point of all the trajectories.

Concentration and deposition are calculated for any particular area (grid square) by assuming that each puff acts independently from all other puffs both from the same source and from other sources. Thus the concentration in a grid square is a simple arithmetic mean of the concentrations for all trajectory segment end points occurring in the grid square. The average is calculated over the total period of time of the trajectory calculations. Such simplified calculations are possible because of the linear relationships in the equations. The average dry deposition for each grid square is calculated as the product of the dry deposition parameter and the average concentration. Wet depositon is calculated for each grid square every time interval then averaged over the total time period.

The reason for the different averaging methods for dry and wet depositon is that k_w and $\bar{k}_w$ vary spatially and temporally, while k_d and $\bar{k}_d$ are each constant and single-valued.

3.1 Deposition Factors

Empirical values from the literature have been assigned to the k factors of deposition and transformation. These are given in Table 1. Each of the k factors represents a simplification of complex physical and chemical processes. Although these are not completely understood, their effects over a long period have been evaluated empirically.

3.1.2 Dry Depositon

Dry deposition is calculated as

$$k_d = \frac{V_d}{H} \quad \text{and} \quad \bar{k}_d = \frac{\bar{V}_d}{H}$$

where V_d and $\bar{V}_d$ are deposition velocities of SO_2 and $SO_4^=$ respectively. Dry deposition depends on the type of surface and the atmospheric stability. The value V_d=1 cm s^{-1} was chosen for the model. Sehmel's (1980) literature survey shows measured values of V_d, the dry deposition velocity of SO_2, under varying conditions of atmospheric stability over grass, water, snow and other surfaces as ranging between extremes of 0.4 to 7.5 cm s^{-1}, with the majority of values lying within the range 1.0 $\pm$ 0.5 cm s^{-1}. Chamberlain's (1980) overview of measured values showed the same wide range as Sehmel, (0.1 to 8 cm s^{-1}) but a somewhat lower representative value, 0.4 to 0.8 cm s^{-1}. Dry depositon of $SO_4^=$ is less than that of SO_2 (e.g. Fisher; 1978). The value $\bar{V}_d$=0.1 cm s^{-1} is used in the model. The mixed layer depth H is constant at 1000 m, representing a long term average value. Possible modifications of the parameters is discussed in section 5.1.

3.1.3 Wet Deposition

Wet deposition factors k_w and $\bar{k}_w$ are loss rates which vary with rain intensity I. For SO_2, the value $k_w = 3. \times 10^{-5}$ I was taken from Summers (1974). This includes both below-cloud washout and in-cloud conversion of SO_2 to $SO_4^=$ with subsequent rain-out. The in-cloud conversion is limited by the rate at which SO_2 is drawn into the clouds, a value estimated (Venkatram et al;1981) as of the order 10^{-5} s^{-1}. Washout of $SO_4^=$ in rain as a long term value is generally considered to be an order of magnitude higher than for SO_2. The value $\bar{k}_w = 3. \times 10^{-4}$ I was used. Further discussion of these relationships is given in section 5.2

3.1.3.1 Deposition in Rain and Snow

Summers' value of k_w for dry snow is an order of magnitude lower than for rain. For wet snow, however, k_w is about 6 times the value for rain, hence a factor of 60 times the value for dry snow. In all cases the snowfall rate is expressed as equivalent rainfall rate. In the model, for preliminary testing of a full year's data, a single value of k_w represents conditions for the year for all grid locations. Snow can occur from November through March over most of the geographical area covered by the array. In the Great Lakes basin, wet snow occurs frequently. Cold dry air flowing over the relatively warmer open water of the lakes in winter gains heat and moisture in the lowest 2 to 3 km. Thus in January and February, while dry snow conditions may prevail north and west of the lakes, periods of wet snow often occur to the south and east of the individual lakes. In simulating a year's data, wet and dry snow conditions were assumed to occur with about equal frequency in winter. The average value of k_w for wet and dry snow is approximately equal to k_w for rain. Hence Summers' rain values for k_w were adopted for the annual simulation.

Measured values of washout coefficients for sulphate, including

dissolved SO_2, have been given by Scott (1981) for winter conditons. The coefficients are widely variable, but some order emerges when he classifies the precipitation as rimed or unrimed snow crystals. Rimed crystals grow primarily by accretion of cloud water droplets on the snow crystal. Unrimed crystals grow by the deposition of water vapour on the snow crystal, when there is very little liquid water in the cloud. The washout rate for rimed (wet) crystals is higher than for unrimed (dry) crystals by a factor of 50 or more. This compares favorably with Summers (1974) values for wet and dry snow which differ by a factor of 60. Scott's work was based on data from 15 winter storms at Muskegon Michigan during the months from November to March. He deduced from the observations that about one half of these consisted of rimed snow and one half, unrimed snow. This result gives some support to our assumption of equal occurrence of wet and dry snow.

3.1.4 Chemical Conversion Rate

The linear rate of conversion of SO_2 to $SO_4^=$ in the model is an oversimplification of a complex process which varies with humidity, the presence of other contaminants and a photochemical effect. Different values of k_t were used for the one month and the full year calculations. A long term average for the year was assumed to be 1% per hour (Newman, 1980). For a one month simulation in summer, when the light intensity is high, k_t=2% per hour.

Similarly, the initial conversion of SO_2 to SO_4, is given different values for the July simulation and for the full year. The value β = 10% takes into account the rapid oxidation due to high concentrations of SO_2 and other chemicals during emission, plus increased photochemical effects in summer. For the initial time step of 6 hours this represents an increase in oxidation rate of somewhat

less than 2% per hour while the pollutant is becoming mixed in the boundary layer. Smith (1981) suggests that during the initial period the amount of $SO_4^=$ in the puff may be in the range 5-30% of the total sulphur. The high value of β used here reflects only a monthly value. The long term average value may be less than this. For the one year simulation β =5%. The value of α is zero.

3.2 Data and Calculations

Input data for the mass balance calculations consist of trajectories as computed in section 2, annual emissions for all source points and precipitation data.

3.2.1. Precipitation Data and Scavenging Calculations

The 1979 precipitation data which we are using was obtained from AES, objectively analysed to the 127 km grid. Precipitation amounts are 24 hour accumulations reported every 12 hours. Where data at a grid point was reported missing we have interpolated in time if (a) there was data at twelve hours before and after the missing time and (b) the two precipitation values were both non-zero or zero. This means that no interpolation was done if rain occurred before and no rain occurred after the missing time, or vice versa.

For a segment end point which occurs at a precipitation reporting time, the value of the precipitation given at that time determines the value of k_w and $\bar{k}_w$ for the trajectory segment. This approach is taken because of the nature of precipitation data. It is the accumulation over the preceding 24 hours. The mass of pollutant has been travelling through this grid square for all or part of the preceding 6 hours. This 6 hour interval occurs within the 24 hour period for which the precipitation is reported. For a segment end point which occurs between precipitation reporting times, the

precipitation value which determines k_w and $\bar{k}_w$ is the next one in time, based on the same reasoning.

3.2.2 Emission Inventory

The emission inventory is the one used by the statistical model (Venkatram et al; 1981). The location and source strengths of 83 sources are shown in Fig. 1. These are annual emissions. The data is a composite of information from several sources. U.S. emission data was compiled from EPA point source inventories (Benkowitz; 1979) and SURE data from the GCA (consulting company contracted by EPRI) major point and area source records. Ontario points were taken from the Ontario Ministry of the Environment sulphur emissions inventory. For the rest of Canada, emission points came from the AES preliminary point and area source inventory (Voldner et al; 1980). Area sources are treated as point sources representing the area.

Trajectory and mass balance calculations are made by the model for 62 of the 83 sources. The remaining 21 sources lie outside the grid array or are too near the boundary for accurate trajectory calculations. Errors in the polynomial calculations occur near the boundaries because of the lack of data for polynomial fitting. Concentration and depositions resulting from the 21 sources as calculated by the statistical model are used as background values for the one year simulation.

Some authors report grouping of sources and calculating representative trajectories for each group as a means of economizing on computer costs. One method (MOE statistical model) is to compute an emissions-weighted mean location for each group, then calculate trajectories from this location. The mass balance along the

trajectories is calculated using the total emissions for the group.

A second method is to compute the geographic mean of the group, calculate trajectories for this location, then translate these trajectories to each emission point within the group for mass balance computations. For each method, care must be taken in grouping the sources. They must be close enough to each other (within one grid interval, 127 km) and in sufficiently similar terrain for the calculations to be valid.

With the purpose of employing the second method, a tentative grouping of the 63 sources into 21 clusters was set up. However, based on a preliminary test of trajectory translation, it was decided not to group the source points for the year 1979, but to compute trajectories for all sources separately. Following this, tests of sensitivity to grouping can be performed using all the 1979 trajectories.

4. Present State of the Model and Future Projections

Both major elements of the model, i.e. trajectory and mass balance calculations have been developed. Results of preliminary tests indicate that the mechanics of the model are working satisfactorily and that predicted concentrations and depositions are the right order of magnitude. Proposed work for the coming months is outlined in section 4.1.

The simulation of one month's data for July 1979 has been used as a base for testing the model parameters. Discussion of the July 1979 simulation is presented in section 4.2. All the trajectories have been calculated for the full year 1979. They have been combined with the gridded precipitation data and stored in such a way that the precipitation data accompanies each trajectory segment. A preliminary simulation of the mass balance for the year has been completed. Results from this first test are presented in section 4.3.

4.1 Proposed Working Schedule

A graphical representation of a proposed working schedule is shown in Fig. 2. Simulations for July 1979 and for the year 1979 represent tests of the model for two different time scales. Gaussian dispersion calculations are included in the shorter time period but not in the longer one. Those tests have been based on a relatively small and imperfect set of meteorological data.

4.1.1 Data

We now have a considerably larger meteorological data set for the year 1978. This is being processed to put it into suitable form for basic input data. Simulation for the year 1978 will then be carried out. This will include the calculation of averages on the annual time

scale with tests on seasonal, monthly and possibly episode (about 4 days) scale.

Planned acquisition of an improved meteorological data set for 1979 and for 1980 plus use of the meteorological data being stored continuously on the Eclipse computer beginning in the latter half of 1980 will permit simulations for the years 1979, 1980, 1981 and future years.

Some adaptations of the model to the 1978 data are necessary. An increased grid area is possible because of improved geographical coverage in the meteorological data. Data is hourly from Canadian stations and 3-hourly from U.S. stations, as opposed to the 6-hourly data used in the calculations for 1979. For 1978 precipitation data is also different. It is descriptive rather than quantitative. Precipitation is classified as to rain or snow, continuous or showery and is described as light, medium or heavy in these categories.

Measured values of concentrations and depositions are necessary for comparison with model results in order to evaluate the model's performance. These are being assembled. They are obtained from many diverse measuring networks in Canada and the United States. These networks have developed independently and for different purposes. In consequence the types of data and their presentation are quite varied. It will take time to organize their data for comparison with the model. However, preliminary comparisons can be made using parts of the data.

4.1.2 Model Parameters

Testing and modification of mass balance parameters is a continuing process in model development. The parameters values are taken from the literature. They include results of measurements and

values derived from theoretical considerations. These are subject to continuous review and testing. Laboratory measurements do not always transfer well to the field. On the other hand field measurements are subject to many difficulties and are very expensive to carry out. Also, values derived under one set of meteorological conditions may be appropriate only to those conditions. Thus parameter values are not well known. Modelling makes use of results of research in representing physical and chemical interactions. It also contributes to an understanding of these processes by providing a different type of experimentation in which the numerous parameters may be tested.

4.1.3 Nitrogen oxides

Use of the model has been proposed to simulate the transport of the oxides of nitrogen. These pollutants undergo more complex chemical reactions in the atmosphere than sulphur oxides. Hence the use of linear equations in the model is even less applicable when applied to sulphur. It may be possible to apply it as a first approximation, with subsequent suitable refinements.

4.2 One Month Simulation

Average ambient SO_2 and $SO_4^=$ concentrations and wet and dry depositions have been computed for the month of July 1979. This is for the 62 emission sources within the grid. Calculations and results for the single month's data are described in the following sections. These are preliminary results. Considerable testing with variations in the model parameters will be necessary before the model can be considered valid.

Modifications of model calculations are necessary when the

model, which is designed for long term calculations (1-2 years) is applied to a shorter time period such as one month. These modifications include a change in the value of the initial conversion β and of the hourly conversion rate k_t as discussed in section 3.1. In addition, the introduction of horizontal dispersion calculations is an important modification for a one month simulation.

4.2.1 Horizontal Dispersion

Because of the relatively small number of trajectories in a one month simulation (about 120 per source for 6-hour intervals), the mass of pollutant is not distributed sufficiently broadly by the variation in trajectory paths. As a result, concentrations show large discontinuities between neighboring grid squares. For the purpose of smoothing, horizontal dispersion has been applied, expanding each puff in time as it moves along the trajectory. The result is a set of 'fuzzy' trajectories. The use of 'fuzzy' trajectories enables us to obtain better averages than would be obtained from individual trajectories. Ideally one should average over several years for the same month. The 'fuzzy' trajectory reflects approximately the variability of a single trajectory from year to year. Horizontal dispersion spreads the centre line concentration and deposition values over several grid squares. A normal or Gaussian distribution has been assumed for each puff such that the concentration C at a point x, y and time t is related to the centre line mass Q' by the equation

$$C(x,y,t) = \frac{Q'(\bar{x},\bar{y},t)}{H} \cdot \frac{1}{2\pi\sigma_x\sigma_y} \exp\left[\frac{-(x-\bar{x})^2}{2\sigma_x^2} - \frac{(y-\bar{y})^2}{2\sigma_y^2}\right] \qquad (7)$$

Assuming $\sigma_x = \sigma_y = \sigma$, the puff radius is 2σ.

Assigning an inital value $\sigma_o = 0.25$ grid interval,

$$\sigma = (\sigma_o^2 + K_D t)^{1/2} \qquad (8)$$

where K_D is the diffusivity coefficient. The value $K_D = 10^5$ $m^2 s^{-1}$ simulates sub-grid wind fluctuations on the meso-scale plus the effect of vertical wind shear in creating horizontal wind variations at different levels in the vertical, as discussed by Smith (1979). This is intermediate between values of $K_D = 10^6$ and $10^7 m^2 s^{-1}$ derived empirially for synoptic scale trajectory variations by Murgatroyd (1969) and Durst et al (1959), and 10^4 m^2 s^{-1}, employed by Bhumralkar et al (1980) for meso-scale diffusion. For $K_D = 10^5$ m^2 s^{-1} the puff is spread over a width of approximately 3 grid squares at t=6 hours and 9 grid squares at 48 hours.

4.2.2 Model results

Concentration

In Figs. 3 and 4 which are plots of computed SO_2 and $SO_4^=$ concentration, high values of SO_2 and $SO_4^=$ concentrations generally correlate with source areas. Due to the large value of k_w for SO_2, the ambient concentration of $SO_4^=$ in the model is influenced strongly by its initial value. Thus this result is not surprising. Two maxima of 30 $\mu g\ m^{-3}$ of SO_2 occur in the Ohio River valley. Near Sudbury Ontario the model computes a maximum SO_2 concentration of 20 $\mu g\ m^{-3}$. The 5 $\mu g\ m^{-3}$ line encloses an area encompassing most of the central northeastern states and the area of southern Ontario close to the lower Great Lakes.

Concentration of $SO_4^=$ varies more smoothly than SO_2, because of the continuous conversion along the trajectories. The two $SO_4^=$ concentration maxima in the Ohio River valley are 10 and 15 $\mu g\ m^{-3}$. A maximum in the Sudbury area exceeds 6 $\mu g\ m^{-3}$. The 3 $\mu g\ m^{-3}$ line encompasses the northeastern states, southern Ontario and reaches northward to the area around Sudbury and into Quebec.

Table 2 compares $SO_4^=$ concentration values computed by the model with measured values for specific sites monitored by the MOE network in Ontario and the SURE network in U.S. The locations on the grid array were chosen by eye and are judged to be within $\pm$ ½ grid distance of each site. Locations are shown in Fig 9. A constant background of 2 $\mu g\ m^{-3}$ has been added to computed concentrations. Recorded $SO_4^=$ concentrations from the MOE network were corrected for spurious high readings which result from conversion of SO_2 to $SO_4^=$ on the Gelman AE glass filters used in the HIVOL monitors. The error is estimated by Lusis (1981) as +6 to +7 $\mu g\ m^{-3}$ and by Stevens (1981) as +3 to +4 $\mu g\ m^{-3}$. Based on these findings a constant factor of 5 $\mu g\ m^{-3}$ was substracted from all MOE monitored values, as shown. SURE measured data were taken from an analysis by Niemann (1980). These are for July 1978 and hence are not directly comparable to computed July 1979 values. But they should provide some indication of the appropriate concentrations.

The model tends to overpredict SO_4 concentrations near the sources, such as at #1 Sudbury, #5 Detroit and #16 and #17 in Illinois. Away from the source areas, concentrations are underpredicted. This may be due in part to localized small sources, possibly an important factor for urban monitoring sites such as Toronto and Hamilton. One of the reasons for the low computed values in New York state is the exclusion from the model of sources just to the east in neighboring states. Also, if the trajectory is dry, i.e, no precipitaiton scavenging occurs, there is likely to be sulphur still in the air at the end of 48 hours. This suggests that, if trajectories were to be extended to a longer period, e.g. 72 hours, the sulphur would be transported farther to the points remote from the sources.

Wet Deposition

Accumulated wet deposition of total sulphur for the month as computed by the model is plotted in Fig. 5. Maximum values exceeding 4,000 u mole m^{-2} occur in the states adjacent to the major source areas. The location of this area of maximum deposition appears to be in agreement with reality (MAP3S/RAINE; 1980). Wet deposition exceeding 1,000 u mole m^{-2} is computed for the wider area of all the central states of the northeastern U.S., all of southern Ontario, projecting into northern Ontario and Quebec. Table 3 shows computed wet deposition of sulphur compared with amounts observed at MAP3S monitoring sites for the month of July, 1979 (MAP3S/RAINE: 1980) in the U.S. and the APN network (Barrie; 1981) in Canada. Where computed values differ signficantly from observed, they tend to be low, especially at sites which are far from the source areas such as Whiteface Mt. (# A), Ithica (#B) and Ela-Kenora (# H). As in the case of the concentration the scarcity of trajectories through distant grid squares for a single month simulation is one contributing factor to these low values. Another is the omission of sources outside the grid, e.g. east of New York State and west of northern Ontario. Wet depositon is overpredicated at Penn State (# C), Charlottesville (# D) and Long Point (# I) near the source areas. Oxford (# G) shows a high predicted wet deposition, but not as high as observed. However, the observed value is unusually high at this site. Possibly this is due to a very localized source, ($\sim$50 km) which the model cannot duplicate.

4.3 One year simulation

The first tests of the model for a full year's data gave results which are discussed below. These must be regarded as preliminary results since there has been no tuning of the model to a full year of meteorological data. With the relatively large number of trajectories for a year, their variations provide horizontal dispersion. So no additional dispersion was applied such as the Gaussian distribution for the one month simulation.

4.3.1 Model results

The computed annual concentration of SO_2 is shown in Fig. 6. Two maxima exceeding 40 $\mu g\ m^{-3}$ occur in the Ohio valley near the source regions and a maximum also occurs at Sudbury. The 5 $\mu g\ m^{-3}$ isopleth encloses much of the central area of the northeastern states, extending into Ontario.

Fig. 7 shows the computed annual concentration of SO_4. The background value of 2 $\mu g\ m^{-3}$ has been added. This represents a generally accepted value of ambient sulphate from natural sources plus small distant anthropogenic sources not included in the emission inventory. In addition, concentrations and wet depositions resulting from the 21 sources not included in the model were computed by the statistical model and added. As may be expected, the SO_4 concentrations do not show the steep gradients that the SO_2 isopleths exhibit. The smooth variation of SO_4 values is in agreement with observations (see Table 5). Maxima in excess of 10 $\mu g\ m^{-3}$ are computed for the source areas. The 6 $\mu g\ m^{-3}$ isopleth encloses the central northeastern states and extends into southwestern Ontario, with a 6 $\mu g\ m^{-3}$ maximum near Sudbury.

In Table 4, computed annual sulphate concentrations are

compared to measured values. The SURE values from U.S. monitors were analysed by Niemann (1981) for the period August 1977 to June 1978. Although this is a different time period than the modelling period, the values from the Niemann analysis should give an approximation of the concentrations for 1979. MOE measured data had a correction factor of -5 $\mu g\ m^{-3}$ applied as for the July data. In the MOE measured data, Toronto and Hamilton reported daily more than 70% of the year. Sudbury reports were daily for July and August, but only every six days for the rest of the year, with a sample size of 76 days for the year. Measured annual concentrations are lower than for the month of July. This might be expected since SO_4 concentrations usually peak in summer. Computed annual concentrations are more evenly distributed from site to site than they were for July alone. This is due to the variations in the many trajectories computed for the full year. Good agreement is shown between computed and observed values. The range of the Ratio: Computed/Measured is from 0.7 to 1.8. Near the source areas, the concentration is overpredicted. This is evident in the Ratio column where #1 Sudbury has a value 1.8, #5 Detroit, 1.3, #16 Illinois, 1.6 and #17 Illinois, 1.8. All other ratios are near 1 or less than 1, the lowest being at Toronto and Hamilton with values of 0.7.

Wet Deposition

The computed pattern of wet deposition of total sulphur in Fig. 8 shows a broad maximum in the Ohio valley extending into southwestern Ontario, with a smaller maximum near Sudbury. Comparison with measured values in Table 5 shows good general agreement between observed and model values. At sites distant from the major sources areas, e.g.. Whiteface, Ithica, Ela-Kenora and Chalk River, wet deposition is underpredicted as in the July case.

Underprediction occurs at Oxford Oh. where the observed value is quite high. As in the July observations, this may result from a localized source.

5. Future Modifications of the Model

After the calculations for 1979 and 1978 have been completed there should be a review of the model results to assess the strengths and weaknesses in the model simulations.

Since the trajectory calculations form the basic unit of the model, it would be well to examine these first. Comparison with examples of 850 mb. trajectories can provide insight into the relative merits of using surface and upper air data for these computations. Calculation of the deviation of the boundary layer wind from geostrophic values due to surface friction and stability effect merits further consideration. Possible modifications to these calculations is discussed in section 5.1.

Having the collection of trajectories as a base, the mass balance calculations can be examined to determine how parameterization can be improved. Wet deposition is of primary concern, because of its influence on concentration calculations and because of the difficulties in parameterizing its effect. These problems arise from cloud physics and chemistry and because rain occurs unevenly on spatial and temporal scales which are not resolved by the model. Possible modifications to wet deposiiton calculations are outlined in section 5.2.

Dry deposition and the changes in its parameters are discussed in section 5.3. Possible changes in the calculation of transformation of SO_2 to $SO_4^=$ are given in section 5.4.

Tests of sensitivity of the model to changes in the parameters should be performed before any new complexities are introduced. The parameters are frequently based on chemical and physical influence in the atmosphere which are not well understood and which

in addition, are difficult to formulize in a simplified manner. Hence their effects on model results should be assessed before adopting then.

After the model has been tested as described above, it can be applied to data now being accumulated on the Eclipse computer for 1981 and later.

Some efforts can be directed also to calculating atmospheric transport of nitrates. The source inventory will have a different form in that the nitrogen emissions are mostly from vehicles on highways. In addition, the atmospheric chemistry of nitrogen is probably less well simulated by linear interactions. However this can be attempted as a first approximation.

Finally, it has been suggested that it may be possible to design an advanced statistical model based on the form of the present statistical model, using trajectory statistics from the Lagrangian model. A consideration of this idea will be given at a later date.

5.1 Wind in the Boundary Layer

Instead of varying the wind speed and turning angle diurnally to parameterize stability effects as is now being done, it is possible to use explicit values of stability for this purpose. The simplest method is to define stability categories based on values of insolation computed from cloud cover data and the angle of incidence of the sun's radiation.

A more complex method of computing wind values directly using similarity principles was devised by Danard (Danard et al; 1980). It is comparable in theory to the calculations of Peterson et al (1981, pp. 17-27) for the Windatlas of Denmark, but differs in practical application. Danard's technique is designed for modelling. It employs an iterative procedure for computing stability parameters using graphs derived by Yamada (1976) from measured values. Input information used by Danard are the wind and temperature at the top of the boundary layer plus, if possible, surface temperature. If this is not available a second iteration scheme is linked to the first. In it the surface temperature is computed from an equation of the energy balance at the earth's surface. Information on incident solar radiation and humidity are needed for this calculation. The two iteration procedures are mutually dependent.

Some adaptation of Danard's method may be possible using surface geostrophic winds computed by the model and estimates of temperature profiles which are typical seasonally.

5.2 Wet Depostion

Three types of modification are suggested here. These are (1) subdivison of a trajectory segment into two parts if it passes from one grid square to another during a time step; (2) simple parameterization of cloud chemistry, (3) incorporation of a representation of the "patchiness" of rain (Smith; 1981).

(1) When a trajectory segment crosses from one grid square to another, the calculation of wet deposition can be broken into two parts using the appropriate k_w and $\overline{k_w}$ values for the two grid squares.

(2). The parameter k_w (or $\overline{k_w}$) can be expressed (Barrie; 1981) as

$$k_w = \frac{WI}{H}$$

where W is a washout coefficient dependent on temperature and the pH of rainwater. To use this in model calculations, it would be feasible to designate typical seasonal temperatures and obtain the appropriate values of W from Barrie's graph of W vs pH for given temperatures. It would be more difficult, however, to define appropriate pH values in the model. A single representative value could be assumed, as a first approximation.

(3) The problem of the "patchiness" of rain arises because of the variability of rain on time and space scales which are smaller than that of the model. Rain clouds are meso-scale ($\sim$10 km) phenomena which cannot be resolved on the 127 km grid. In addition, rain occurrence varies on a time scale of about 15 minutes, whereas the precipitation effect in the model is calculated at 6 hour intervals.

Smith (1981) attempted to solve this problem using statistical methods. For example, for a given location, he determined the probability that there will be no rain in the next 15 minutes, when rain has occurred in the preceding 6 hours. In addition to this type of calculation, he separated the trajectories into wet regions and dry regions, computing statistics of the movement from wet to dry regions and vice versa.

It would appear then that the use of a probability factor p_r might be introduced into the wet deposition computation, making the general formula

$$\text{Wet dep} = p_r \frac{(WI)}{H} C \qquad (9)$$

where C is the concentration, i.e., q or s. Determination of p_r would take into account, in some way, the considerations given above. Concerning the movement of trajectories from wet to dry regions, it may be useful to examine the relative motions of rain clouds and trajectories, by expressing the correlation between boundary layer and cloud level winds. Thus if a trajectory is in a wet region there may be some tendency for it to move with the rain area, thus increasing the value of p_r.

5.3 Dry Deposition

The calculation of dry depsition for both SO_2 and $SO_4^=$ can be generalized for the purpose of this discussion as

$$\text{Dry dep} = k_d \cdot \bar{C} = \frac{V_d \cdot \bar{C}}{H}, \qquad (10)$$

where $\bar{C}$ is the layer averaged concentration. Both V_d and H currently are assigned fixed values.

In reality V_d and H both vary with thermal stability and the type of surface, e.g. vegetation type and water surface. Also the appropriate concentration is not $\bar{C}$ but the surface value C_o.

It should be noted here that there is a tendency for the model to be insensitive to changes in dry deposition. This is because of the compensating relationship which exists between k_d and $\bar{C}$. If k_d is made smaller, then downstream values of $\bar{C}$ are greater. Hence the product $k_d.\bar{C}$ does not change as much as the terms taken individually. Consequently complicated calculations may not be justified in the search for representation of reality here.

5.3.1 Deposition velocity

Sheih et al (1979) have produced maps of variations is V_d based on land use. These values could be incorporated into the model. The overall range of values for V_d is from 0.1 to 1.6 cm s^{-1}. These values were obtained from field measurements for varying surface types and

atmospheric stabilities. A survey of the literature by Sehmel (1980) shows that values of V_d measured by many different authors is within this range, with some extreme values ranging as low as 0.04 and as high as 7.0. Values for snow surfaces may have to be added to Sheih's tables which assume midsummer conditions. These have been measured by Whelpdale and Shaw (1974) and Barrie and Walmsley (1978).

5.3.2 Mixed Layer Depth

The height to which surface mixing is effective rises in the daytime when the heated surface warms the lower atmospheric layers and lowers at night when the surface cools. This effect can be included in the model by diurnal variation of H. A more explicit calculation of H can be based on values of stability calculated from cloud cover and the sun's angle. When a trajectory moves into a region of lower H value, some of the mass of the pollutant remains above the boundary layer. The model will then suffer loss of mass at the upper boundary due to this effect, unless the mass is recaptured when the value of H is higher.

5.3.3 Surface Concentration, Vertical Dispersion

When dry deposition is expressed in terms of surface concentration C_o, as opposed to the layer-average value C, then the time rate of change in concentration is expressed by the diffusion equation in the vertical,

$$\frac{\partial C}{\partial t} = \frac{\partial K_z \frac{\partial C}{\partial z}}{\partial z} + \text{SOURCES} + \text{SINKS} \quad (11)$$

and boundary conditions

$$\frac{\partial K_z \frac{\partial C}{\partial z}}{\partial z} = 0 \quad \text{at } z=H \tag{12a}$$

$$\frac{\partial K_z \frac{\partial C}{\partial z}}{\partial z} = \frac{V_d . C_o}{H} \quad \text{at } z=0 \tag{12b}$$

For SO_2 the SINK terms in equation (11) express deposition (dry and wet) and transformation to $SO_4^=$; for $SO_4^=$ the SINK terms are the depositions only. The point source for SO_2 is located either at ground level or elevated a fraction of the boundary layer height. There are two source terms for $SO_4^=$, the point source and the source due to chemical conversion from SO_2 and hence proportional to the transformation loss term of the SO_2 equation.

Shannon (1981) integrates equation (11) numerically, using several vertical levels. Fisher (1975) and Maul (1977) have solved equation (11) analytically for constant k_z over the boundary layer, taken either as a whole or in parts. The near surface values of k_z are of primary importance in the calculation of deposition. Above 50-100m, k_z can be considered a constant for long range transport calculations. Either a numerical solution such as Shannon's or an analytical solution could be used in the model to simulate the vertical concentration distribution, with attention directed to the near-surface values. As previously noted, it is important to test the sensitivity of the model to the range of possible values of C_o before embarking on this type of complication in the model process. A simple adjustment in the value of V_d may be found to be sufficient.

Graphs of variation of concentration with height as obtained from the analytical solution by Maul (1977) show that beyond 100 km the concentration is distributed almost evenly in the vertical, except

in the lowest 50 m. Near the surface the ratio C_o/C = 0.6 when V_d=1 cm s^{-1}. Graphs by Scriven and Fisher (1975) of C_o vs distance from the source, for values of V_d from 0.1 to 5.0 cm s^{-1} show modified exponential decay of C_o with distance. An almost linear decrease of C_o with increasing values of V_d illustrates the compensating relationship between the two parameters.

5.4 Transformation of SO_2 Sulphur dioxide to Sulphate

Photochemical effects on the rate of conversion can be represented by diurnal and seasonal changes in k_t or by a dependence on cloud cover and the sun's angle. The conversion rate appears to increase in rain. Thus k_t could be increased for wet sections of the trajectories. Transformation also has a dependence on the concentration of $SO_4^=$ and this is more difficult to calculate because it makes eq. (1) non-linear. It may be possible to introduce an iterative calculation for this process. This can be tried, obtaining a first value of concentration, then running the model repeatedly with k_t adjusted to the previously obtained concentration each time.

6. Conclusion

The Lagrangian model which has been described in this report constitutes a significant departure from the statistical model, in that the motion and the state of pollutant is calculated step by step during transport along trajectories. Over a long period of time these trajectories may be considered collectively as a statistical ensemble. The mean trajectory and standard deviation may then be regarded as the centre line of the path of the pollutant and the large scale horizontal diffusion. This is in contrast with the statistical model which assumed these values at the outset. Where the statistical model assumed single values for calculating mass decay and conversion, in the Lagrangian model an attempt is being made to simulate temporal and spatial changes in these factors. The Lagrangian model consumes much more computing time and hence is a great deal more costly to run. Because of the interactions among the various components, the results of changes in the model cannot be anticipated with certainty. So sensitivity tests are necessary before incorporating these changes.

Such influences as occurrence of rain, small variations in the winds and the chemical changes in the pollutant cannot be defined precisely at each step. This means that the trajectories, concentrations and depositions calculated by the model must be averaged over a period of time to be considered valid.

The basic form and mechanisms of calculation of the model are now satisfactorily developed. However, considerable testing and adjustments are necessary before model predictions can be regarded with confidence.

REFERENCES

Atmospheric Model Development Unit, 1980: Lagrangian model of long range transport of sulphur oxides; draft internal paper.

Barrie, L.A., 1981: The prediction of rain acidity and SO_2 scavenging in eastern North America; Atmos. Envir. 15, 31-41.

Barrie, L.A. and J.L. Walmsley, 1978: A study of sulphur dioxide depostion over snow; Atmos. Envir. 12, 2321-2332.

Barrie, L.A., 1981; Environment Canada's Long range transport of atmospheric pollutants program: Atmospheric studies; Report AWRB-81-021-T.

Benkowitz, G., 1980: Compiling a multistate emissions inventory, Brookhaven National Laboratory/MAP3S Report, BNL-26843, Atmospheric Sciences Division, Dept. of Energy and Environment, Brookhaven Nat. Laboratory, Upton, New York, U.S.A.

Bhumralkar, C.M., R.L. Mancuso, D.E. Wolf, R.A. Theuillier, K.C. Nitz and W.B. Johnson, 1980: Adaptation and application of a long-term air pollution model ENAMAP-1 to eastern North America, Final report, contract 68-02-2959, SRI International, Menlo Park, California.

Danard, M., G. Ellenton and H. Sahota, 1980: Computing temperatures and winds at the earth's surface, Part 3, Techniques for Calculating low-level winds and temperatures; contract serial no. 1SZ78-00219 for Atmospheric Environment Service, Downsview, Ontario.

Durst, C.S., A.F. Crossely and N.E. Davis, 1959: Horizontal diffusion in the atmosphere as determined by geostrophic trajectories. J. Fluid Mech. 6, 401-421.

Eliassen, A. and J. Saltbones, 1975: Decay and transformation rates of SO_2 as estimated from emission data, trajectories and measured air concentrations; Atmos. Envir. 9, 425-429.

Fisher, Bernard E.A., 1978:
Long range transport and despition of sulfur oxides; Central Electricity Research Laboratories, Leatherhead, Surrey, United Kingdom.

Maul, P.R., 1977: The mathematical modelling of the meso-scale transport of gaseous pollutants; Atmos. Envir. 11, 1191-1195.

Lusis, M. 1981:
Sulfate monitoring in the NAPS network; internal memorandum, Air Resources Branch, Ontario Ministry of Environment.

MAP3S/RAINE Resarch Community, 1980:
The MAP3S precipitation chemistry network: statistical overview for the period 1976-1980; U.S. U.P.A. and U.S. Dept of Energy cotnract #DC-AC06-76 RLO 1980.

Murgatroyd, R.J., 1969:
Estimations from geostrophic trajectories of horizontal diffusion in the mid-latitude troposphere and lower stratosphere. QJRMS 95, 40-62.

Newman, L., 1980; Atmospheric oxidation of sulphur dioxide; Ch. 7, Atmospheric Sulfur Deposition, Environmental Impact and Health Effects; ed. by David S. Shriner, Chester R. Richmond, Steven E. Lindberg. Ann Arbor Science pub. 131-144.

Niemann, Brand L., 1980:
Initial data base for intercomparison of regional air quality simulation models: Part 1 Ambient sulfur dioxide and sulfate concentraitons in eastern North America during 1977 - 1978, (draft). Office of environmental engineering and technology, U.S. EPA, Wash. D.C. 20460.

Petersen, E.L., I. Troen and S. Frandsen, 1981: Danish Windatlas, rational method of wind energy siting; Riso Nat. lab., DK-4000 Roskilde, Denmark; 229 pages.

Pettersen S., 1956: Weather analysis and forecasting, p. 27, McGraw-Hill, New York.

Scott, B.C., 1981: Sulphate washout ratios in winter storms. Jour. Appl. Met., 20, 619-625.

Scriven, R.A. and B.E.A. Fisher, 1975: The long range transport of airborne material and its removal by deposition and washout-II. The effect of turbulent diffusion; Atmos. Envir. 9, 59-68.

Sehmel, George A., 1980: Particle and gas dry deposition: A review; Atmos. Envir. 14, 983-1011.

Shannon, Jack D., 1981: A regional model of long term sulphur atmospheric pollution, surface removal and net horizontal flux. Atmos. Envir. 15, 689-701.

Shieh, C.M., M.L. Weseley and B.B. Hicks, 1979: Estimated dry deposition velocities of sulfur over the eastern United States and surrounding regions; Atmos. Envir. 13, 1361-1368.

Smith, F.B., 1979:
The character and importance of plume lateral spread affecting the concentration downwind of isolated sources of hazardous material. WMO Symposium on the long range transport of pollutants and its relation to general circulation including stratospheric/tropospheric exchange processes, Sofia, WMO NO.538 241-252.

Smith, F.B., 1981:
The significance of wet and dry synoptic regions on long range transport of pollution and its depositon. Atmos. Envir. 15, 863-874.

Summers, Peter W., 1974: Note on SO_2 scavenging in relation to precipitation type; Precipitation Scavenging, Proc. Symposium, Champaign Ill.; pub. CONF-741003 Nat. Technical Information Service, U.S. Dept of Commerce, Springfield Va. 88-94.

Sykes, R.I. and L. Hatton, 1976: Computation of horizontal trajectories based on the surface geostrophic wind; Atmos. Envir. 10, 925-934.

Venkatram, A., B.E. Ley and S.Y. Wong, 1981: A statistical model to estimate long-term concentrations of polutants associated with long-range transport; Atmos. Envir. 16.

Voldner, E.G., Y. Shah and D.M. Whelpdale, 1980: A preliminary Canadian emissions inventory for sulfur and nitrogen oxides. Atmos. Envir., 14, 419-428.

Whelpdale, D.M. and R.W. Shaw, 1974: Sulphur dioxide removal by turbulent transfer over grass, snow and water surfaces; Tellus, 26, 196-205.

Yamada, T., 1976: On similarity functions, A, B and C of the planetary boundary layer; Jour. Atmos. Sc. 33, 781-793.

TABLE 1

Values of Model Parameters

		July 1979	Year 1979
k_t	SO_2 to SO_4 transformation rate	2% hr^{-1}	1% hr^{-1}
v_d	SO_2 dry deposition velocity	1 cm s^{-1}	
$\bar{v}_d$	SO_4 dry deposition velocity	0.1 cm s^{-1}	
H	mixing height	1000 m	
α	initial deposition of SO_2	0	
β	local oxidation SO_2 to SO_4	10%	5%
Δt	time step	6 hour	
k_w	SO_2 wet depositon rate	$(3 \times 10^{-5})I$	
$\bar{k}_w$	$SO_4^=$ wet deposition rate	$(3 \times 10^{-4})I$	
I	precipitation rate	mm s^{-1}	

TABLE 2

SO_4 CONCENTRATION

JULY 1979

Site Name	#	Model* Value $\mu g\ m^{-3}$	Reading $\mu g\ m^{-3}$	Observed Value Corrected ($-5\ \mu g\ m^{-3}$) $\mu g\ m^{-3}$
			MOE Network July 1979	
Sudbury	1	7.8	12	7
Parry Sound	2	5.2	11	6
Toronto	3	6.6	16	11
Hamilton	4	8.4	16	11
			SURE Network July 1978	
Detroit	5	9.3	8	
Indiana	6	5.1	11	
	7	8.7	12	
	8	8.3	13	
Ohio	9	6.8	14	
	10	7.0	14	
	11	15.4	17	
Penn.	12	8.0	13	
	13	15.5	16	
	14	7.1	12	
	15	9.5	11	
Illinois	16	13.9	10	
	17	11.1	8	
	18	10.0	15	
New York	19	6.6	15	
	20	6.4	10	
	21	5.3	10	
	22	3.8	7	

*Background of 2 $\mu g\ m^{-3}$ included.

TABLE 3

Wet Depositon of Total Sulphur

July 1979

Site Name		#	Model Value	Observed Value
			μmole m^{-2} mo^{-1}	
				MAP3S Network
Whiteface Mt.	N.Y.	A	701	2010
Ithica	N.Y.	B	1960	5340
Penn. State	Penn.	C	4209	3600
Charl.	Va.	D	2142	1710
Urbana	Ill.	E	3970	4140
Lewes	Del.	F	2360	2520
Oxford	Oh.	G	4926	7,700
				APN Network
Ela-Kenora	Ont.	H	32	300
Long Point	Ont.	I	4955	4,000
Chalk River	Ont.	J	1049	4,000

TABLE 4

SO_4 Concentration
Year 1979

Station	Computed**	Measured	Corrected (-5 μg m^{-3})	Ratio
	μg m^{-3}	μg m^{-3}	μg m^{-3}	Computed / Measured
		MOE (1979)		
1. Sudbury	9.5	10.1	5.2	1.8
3. Toronto	5.8	13.5	8.5	0.7
4. Hamilton	6.8	15.0	10.0	0.7
		SURE* (1978)		
5. Detroit	9.1	7.0		1.3
6. Indiana	6.8	7.5		0.9
7. Indiana	8.0	6.9		1.2
8. Indiana	8.0	7.8		1.0
9. Ohio	6.7	5.7		1.2
10. Ohio	7.3	8.8		0.8
11. Ohio	9.1	7.5		1.2
12 Penn.	6.7	6.7		1.0
13 Penn.	9.6	8.0		1.2
14. Penn.	5.3	7.4		0.7
15. Penn.	6.6	7.4		0.9
16. Illinois	9.3	5.6		1.7
17. Illinois	6.0	3.3		1.8
18. Illinois	6.6	6.0		1.1
19. New York	5.7	5.3		1.1
20 New York	5.5	6.1		0.9
21 New York	4.4	5.4		0.8

*Nieman analysis Aug. 1977 to June 1978

**Includes background of 2 ug m^{-3} plus background from 21 additional sources as calculated by statistical model.

TABLE 5

Wet Deposition Total Sulphur

Year 1979

Site Name	#	Model* Value kg ha^{-1} y^{-1}	Observed Value (prorated) kg ha^{-1} y^{-1}
			MAP3S Network 1979
Whiteface Mt.	A	5.7	7.1
Ithica	B	7.6	8.7
Penn. State	C	9.9	9.7
Oxford Oh.	G	5.9	10.4
			APN Network 1979
Ela - Kenora	H	2.9	3.2
Long Point	I	13.3	13.3
Chalk River	J	6.7	11.1
			CANSAP Network 1978
Atikokan	K	3.0	3.5
Kingston	L	6.4	9.1
Peterborough	M	10.2	8.5
Simcoe	N	13.3	13.9

*Background of 2 kg ha^{-1} yr^{-1} included.

GE/mb/AQM9-13

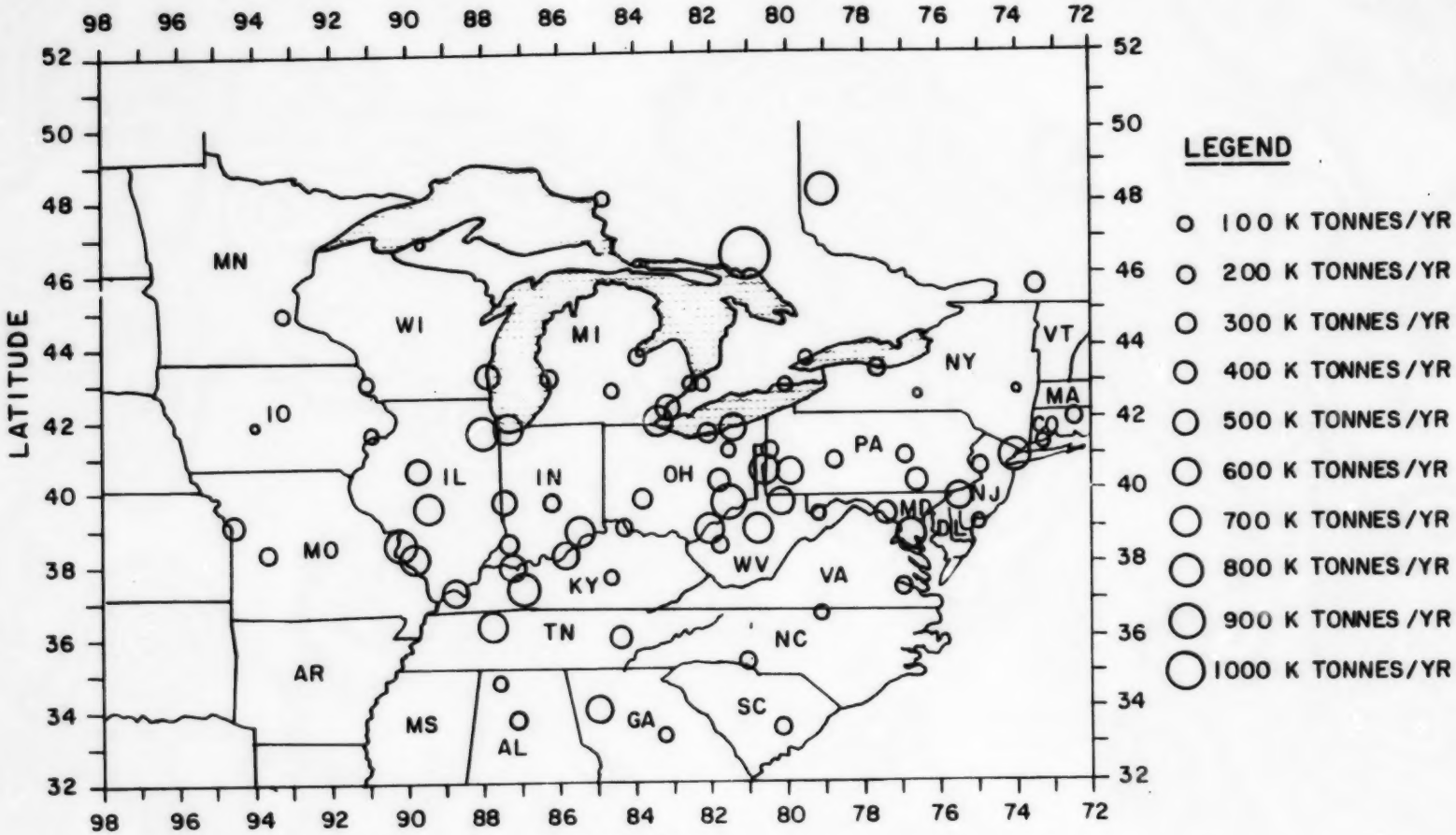

SOURCES OFF THE MAP

EMISS	SOURCE NAME	LAT	LONG	EMISS	SOURCE NAME	LAT	LONG
O	PORTLAND – AUGUSTA	43·4	71·0	O	FLIN FLON MAN	54·9	101·0
O	BOSTON-WORCESTER	40·3	71·3	O	MONCTON N. B.	45·5	66·0
O	NEWPORT-FALL RIVER	41·7	71·1	o	NOVA SCOTIA	45·0	62·8
O	THOMPSON. MAN.	55·4	97·5	o	GASPE BAY QUEBEC	48·6	65·3

Figure 1 : Model Emission Inventory for 1979, Size of Circle Indicates Source Strength

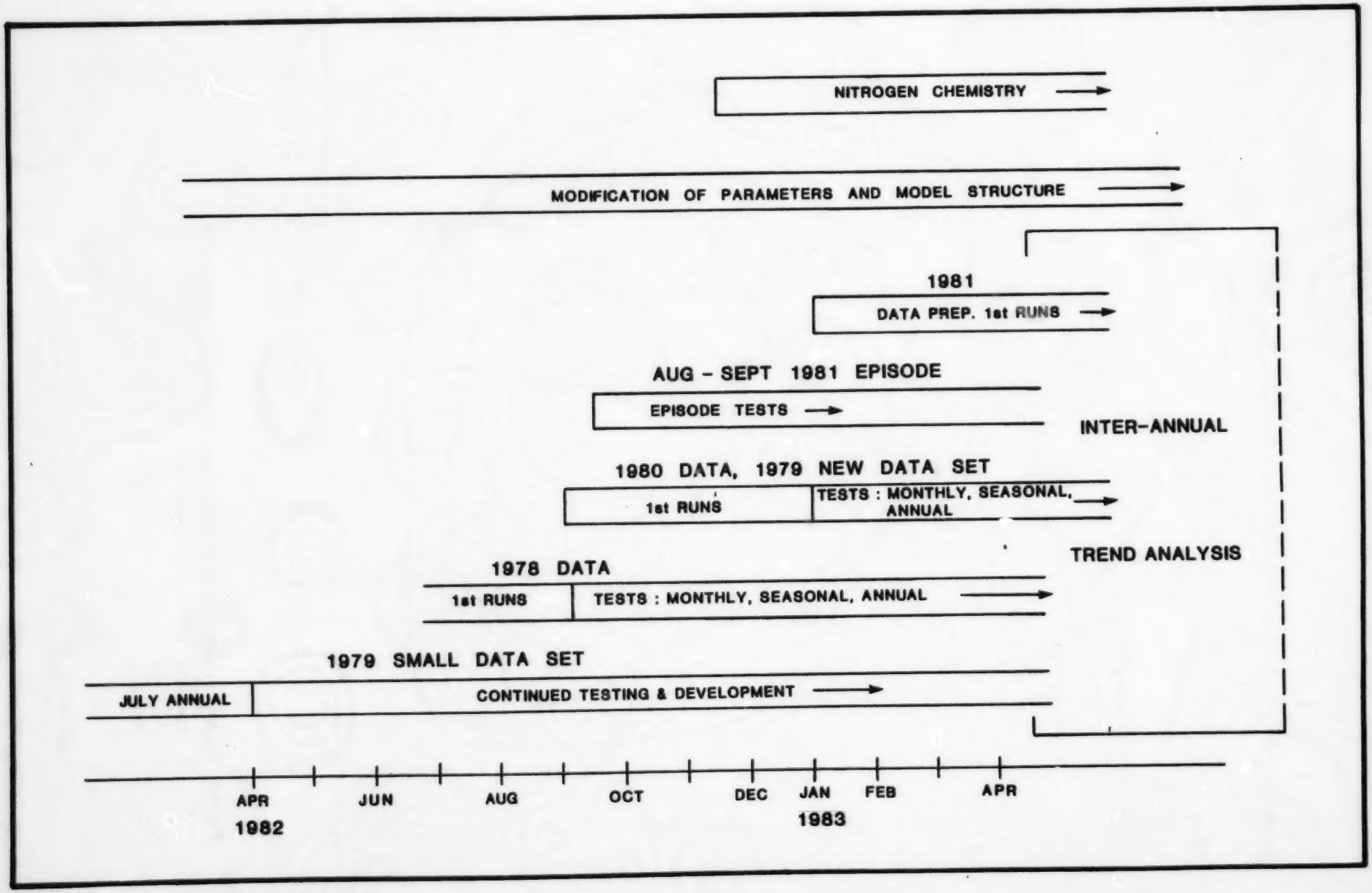

Figure 2 : Proposed Working Schedule

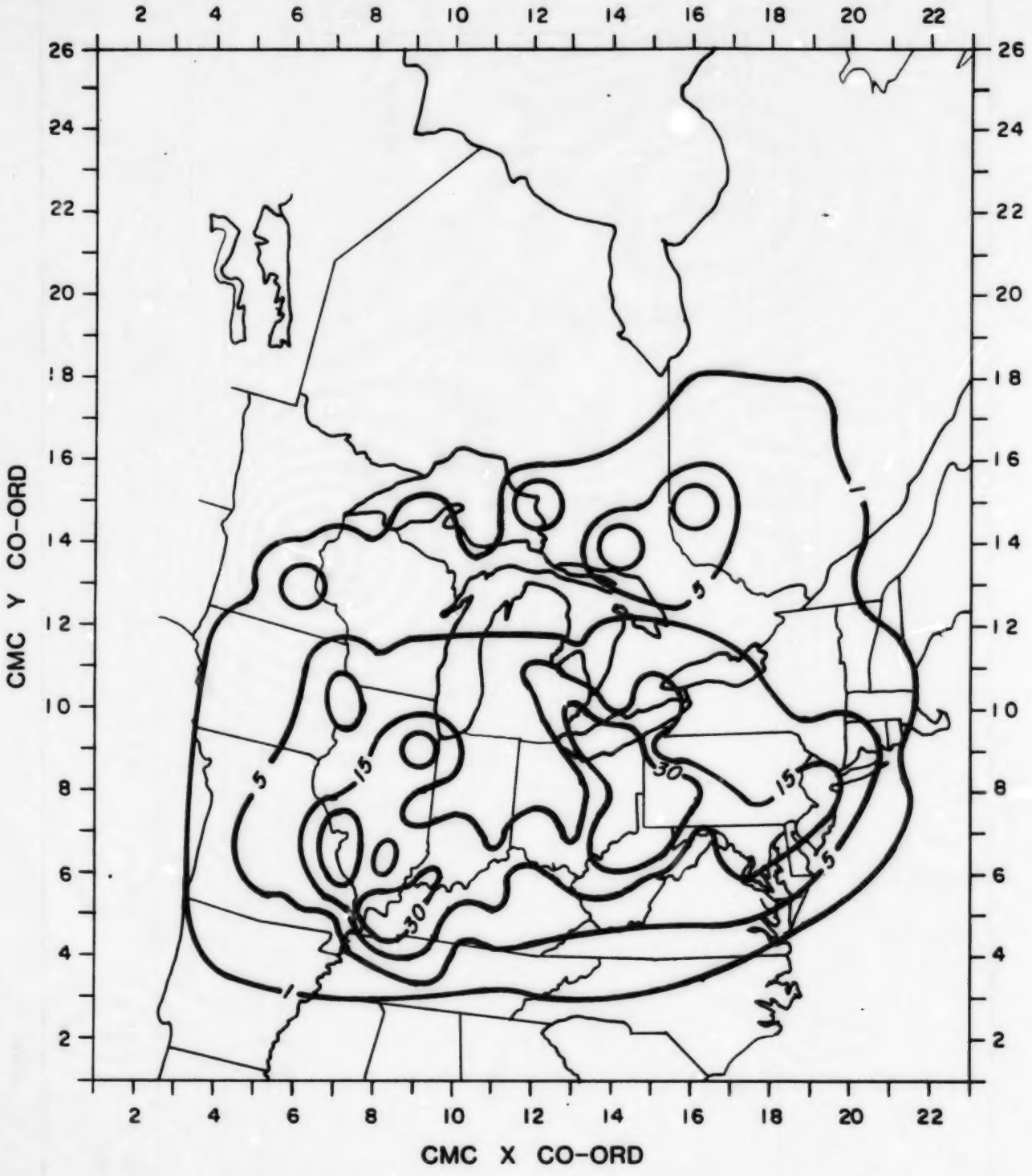

Figure 3 : Model Computed Monthly Average SO_2 Concentration for July, 1979 in $\mu g\ m^{-3}$

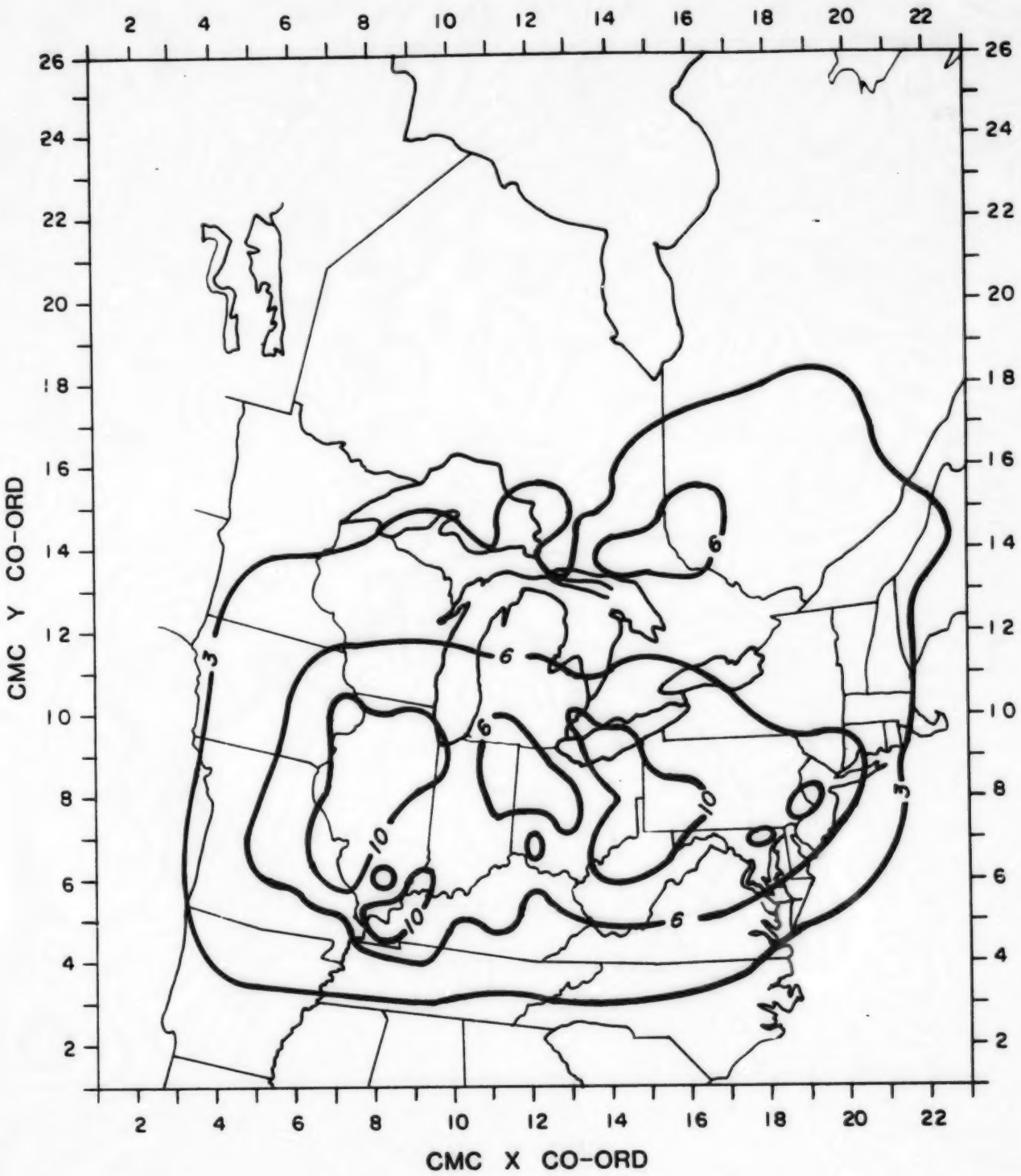

Figure 4 : Model Computed Monthly Average SO_4 Concentration for July, 1979 in $\mu g\ m^{-3}$, Including Background of 2 $\mu g\ m^{-3}$

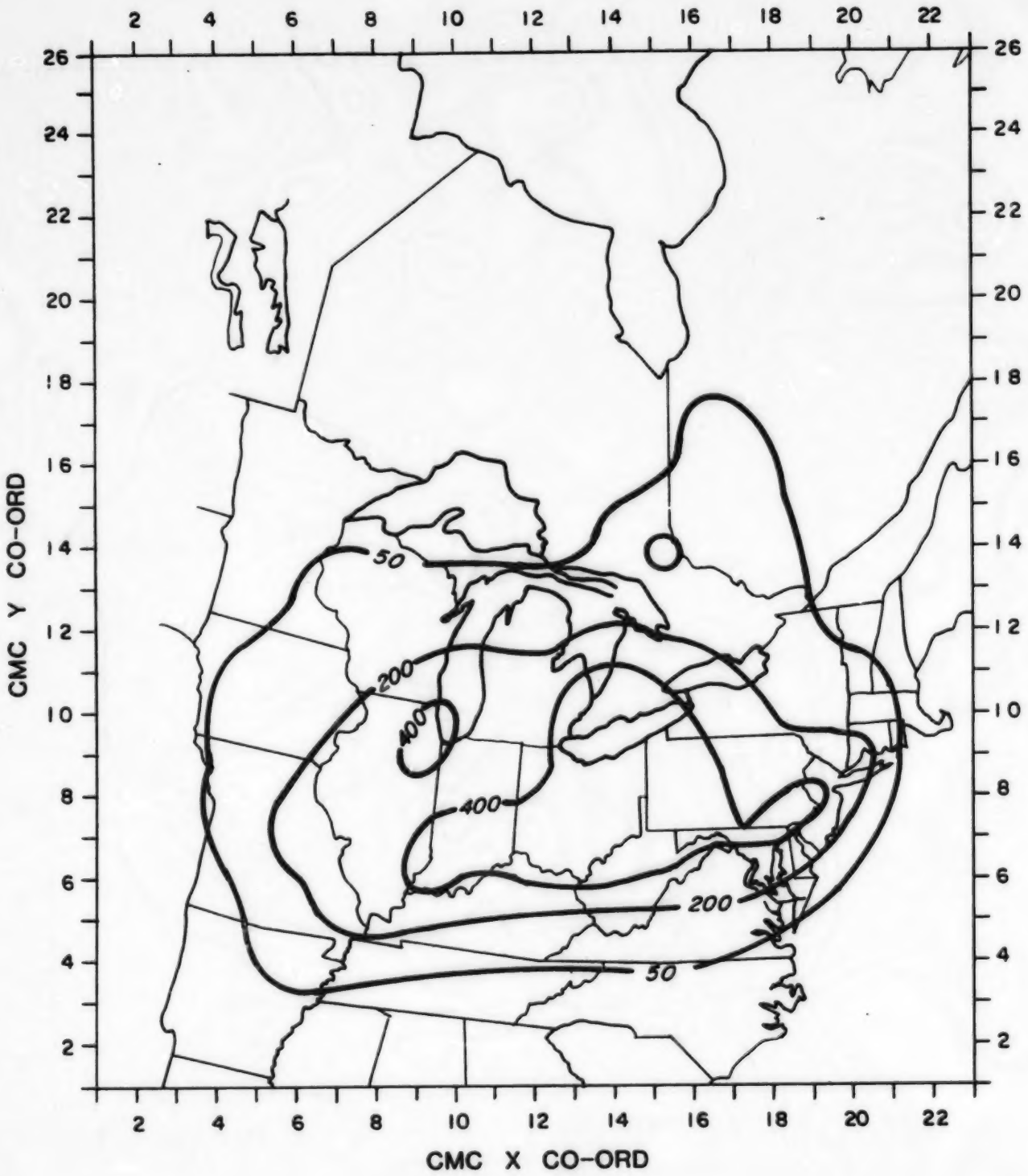

Figure 5 : Model Computed Monthly Accumulation, wet Deposition of Total Sulphur for July, 1979 in Units of 10μmole m^{-2}Month^{-1}

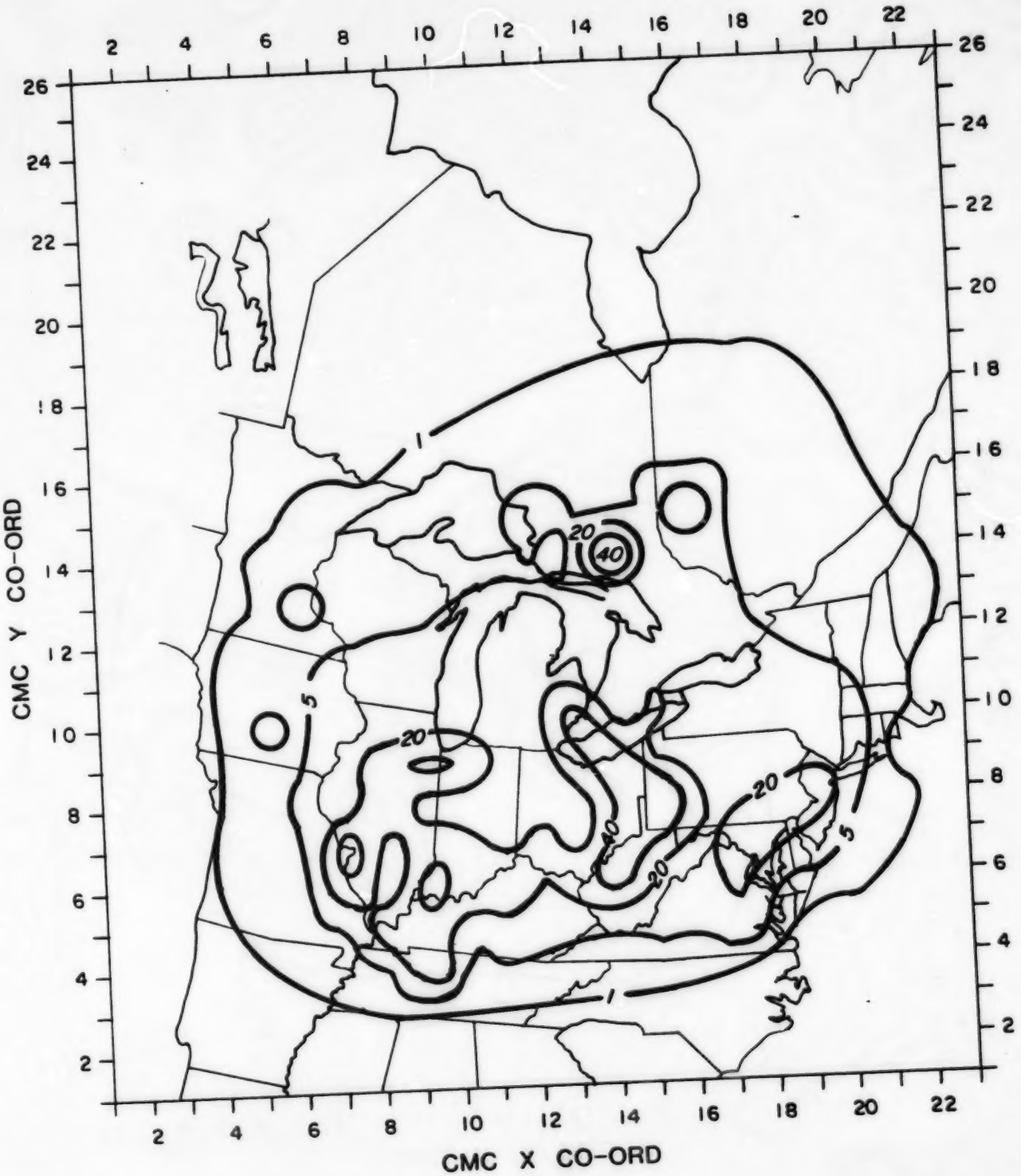

Figure 6 : Model Computed Annual Average SO_2 Concentration for 1979 in $\mu g\ m^{-3}$

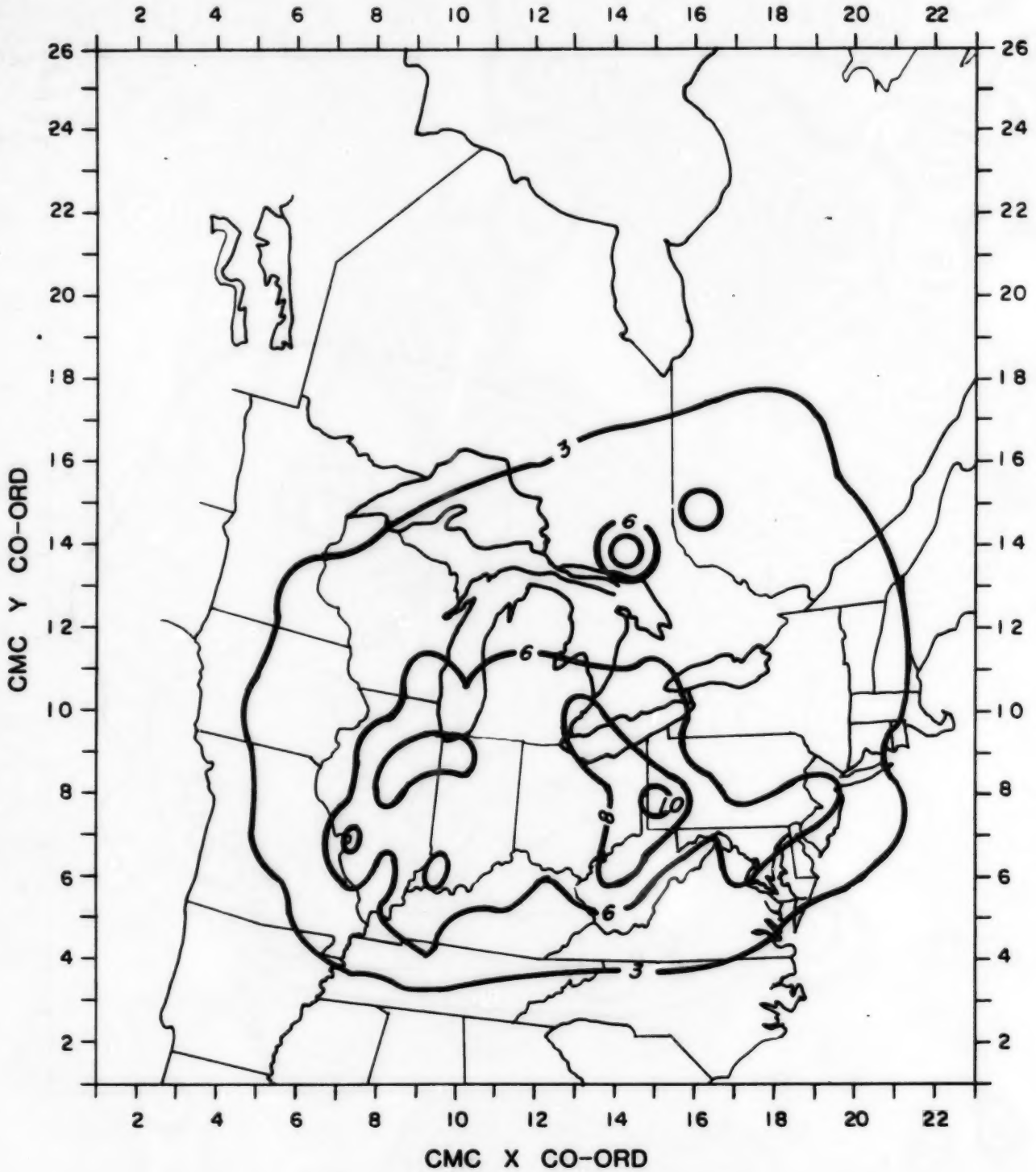

Figure 7 : Model Computed Annual Average SO_4 Concentration for 1979 in $\mu g\ m^{-3}$, Including Background of $2 \mu g\ m^{-3}$

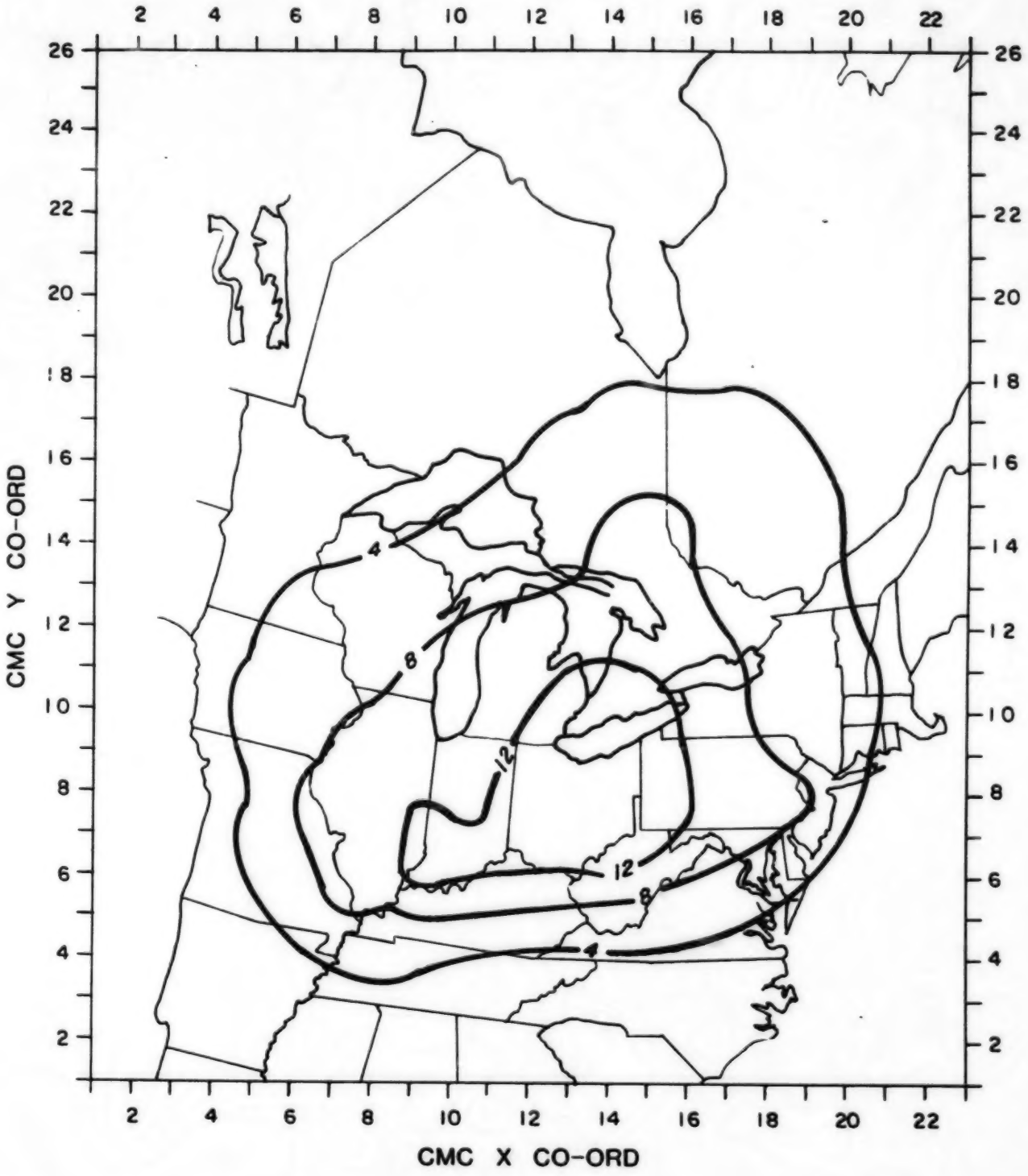

Figure 8 : Model Computed Annual Accumulation, wet Deposition of Total Sulphur in kg ha^{-1} yr^{-1}, Including Background of 2 kg $ha^{-1}yr^{-1}$

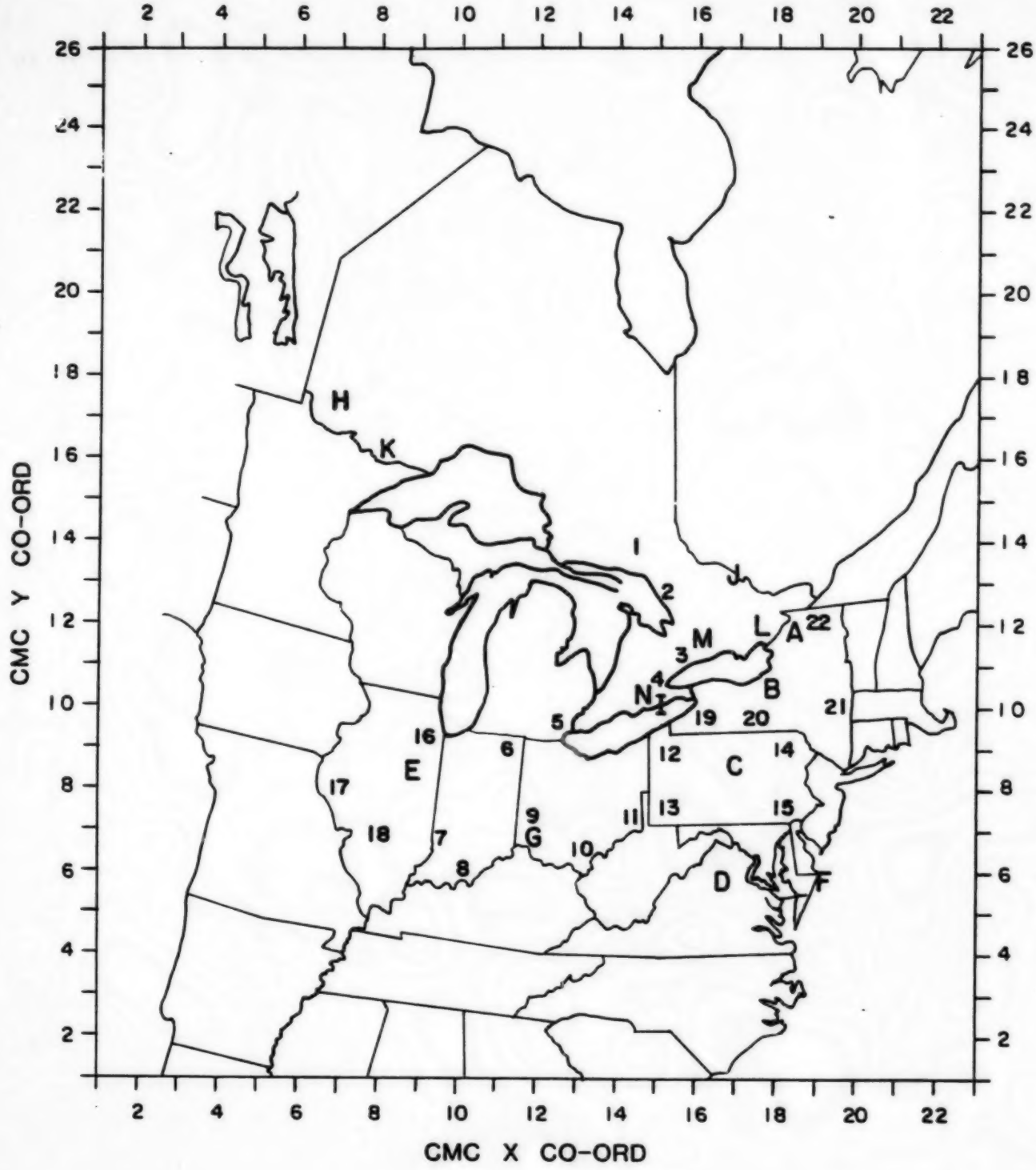

Figure 9 : Locations of Monitoring sites for Ambient Sulphate Concentrations (Marked by Numbers) and Wet Deposition (Marked by Letters)